

# Restricted Analogues Provide Evidence of a Biologically Active Conformation of Thyrotropin-Releasing Hormone

LIISA LAAKKONEN, WENHAO LI, JEFFREY H. PERLMAN, FRANK GUARNIERI, ROMAN OSMAN, KEVIN D. MOELLER, and MARVIN C. GERSHENGORN

Department of Physiology and Biophysics, Mount Sinai School of Medicine of the City University of New York, New York, New York 10029 (L.L., F.G., R.O.), Department of Chemistry, Washington University, St. Louis, Missouri 63130 (W.L., K.D.M.), and Division of Molecular Medicine, Department of Medicine, Cornell University Medical College and The New York Hospital, New York, New York 10021 (J.H.P., M.C.G.)

Received January 17, 1996; Accepted February 29, 1996

## SUMMARY

Thyrotropin-releasing hormone (TRH) is a tripeptide (<Glu-His-Pro-NH<sub>2</sub>) that signals through a G protein-coupled receptor. TRH is a highly flexible molecule that can assume many conformations in solution. To attempt to delineate the biologically active conformation of TRH, we synthesized a pair of conformationally restricted cyclohexyl/Ala<sup>2</sup>-TRH analogues. The diastereomeric analogues use a lactam ring to restrict two of the six free torsional angles of TRH and constrain the X-Pro-NH<sub>2</sub> peptide bond to *trans*. Unrestricted cyclohexyl/Ala<sup>2</sup>-TRH exhibited a 650-fold lower affinity than TRH for TRH receptor and was 430-fold less potent than TRH in stimulating inositol phosphate second messenger formation. One diastereomer exhibited higher affinity and potency than the unrestricted analogue

despite the presence of the methylene bridge and fused ring, whereas the other showed lower affinity and potency. Computer simulations predicted that the positions of the cyclohexyl/Ala<sup>2</sup> and Pro-NH<sub>2</sub> moieties relative to <glutamate were different in the two analogues and that the conformation of the higher affinity analogue is different from that of *trans*-TRH in solution but is superimposable on that of *trans*-TRH found in a model of the TRH/TRH receptor complex. These experimental findings identify a favored relative position of <glutamate and Pro-NH<sub>2</sub> in the more active conformation of two diastereomeric analogues of TRH and provide independent support for the model of the TRH/TRH receptor complex.

TRH is a tripeptide (pyroglutamic acid/histidine/prolineamide, <Glu-His-Pro-NH<sub>2</sub>) that signals through a receptor (TRH-R) (1) that is a member of the G protein-coupled receptor (GPCR) superfamily (2). To understand TRH signaling at the molecular level, it is important to determine the structure of the TRH/TRH-R complex. Because the three-dimensional structure has not been experimentally resolved for any ligand/GPCR complex, models of GPCRs have been constructed (3, 4). We constructed a model of the transmembrane domain of TRH-R (5) based on the analysis by Baldwin of GPCR sequences (6). We used rhodopsin as template (7) to position the lipid-spanning helices (8) and docked TRH into the binding pocket to form a TRH/TRH-R complex based on a number of experimental observations of direct contact points between specific moieties on TRH and individual amino acid residues within TRH-R (5, 9). This model makes predictions regarding the structure of TRH-R and of the conformation of TRH that is present within the receptor binding pocket. Our

hypothesis is that the conformation of TRH in the TRH/TRH-R complex is the biologically active TRH conformation.

Conformations of TRH have been defined in a crystal (10) and in solution (11-15). In all structures resolved experimentally, the peptide backbone is extended and the preferred conformation of the peptide bond between histidine and proline is *trans*, although a small fraction of *cis* structures was found in solution. The relation between the pyrrolidone ring of <glutamate and the pyrrolidine ring of Pro-NH<sub>2</sub>, both of which are important for TRH binding (5, 16, 17), is dependent on four free torsional angles. These angles have been found at two or more values in NMR spectroscopic studies of TRH, attesting to the flexibility of TRH in solution. The conformation of TRH that is biologically active has not been determined experimentally. We describe the design, synthesis, and biological and structural properties of two conformationally restricted analogues of cyclohexyl/Ala<sup>2</sup>-TRH (<Glu-cyclohexyl-Ala-Pro-NH<sub>2</sub>) that provide initial insight into the active structure of TRH.

## Materials and Methods

**Syntheses.** The conformationally restricted analogues of cyclohexyl/Ala<sup>2</sup>-TRH (Fig. 1),  $\alpha$ CH-TRH and  $\beta$ CH-TRH, were synthesized

This work was supported by National Institutes of Health Physician Scientist Award DK02101 (J.H.P.) and Grant DK43036 (M.C.G.).  
L. L. and W. L. contributed equally to this study.

**ABBREVIATIONS:** TRH, thyrotropin-releasing hormone; TRH-R, TRH receptor; GPCR, G protein-coupled receptor.

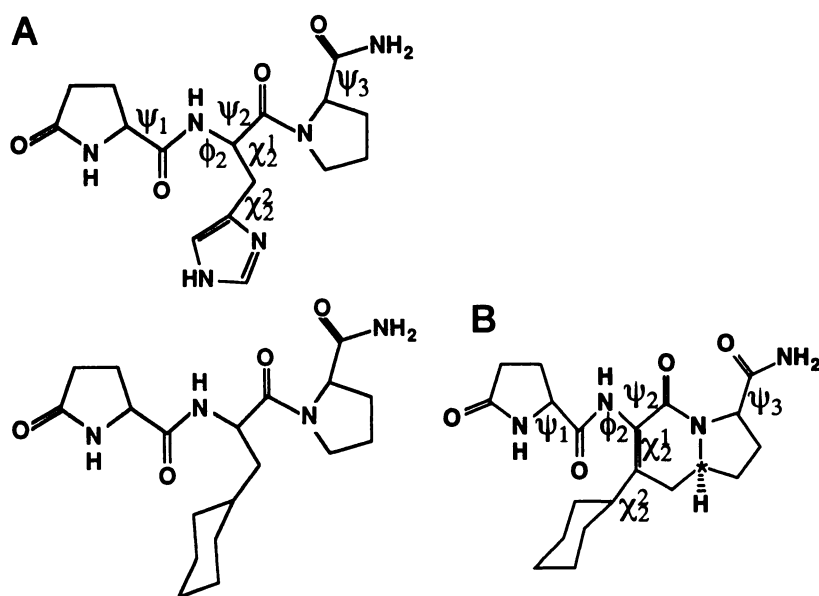


**Fig. 1.** Chemical structures of TRH (A, top), cyclohexyl/Ala<sup>2</sup>-TRH (A, bottom), αCH-TRH (B), and βCH-TRH. B, αCH-TRH [(6S,9S,12S)-1-Aza-3-aminopyroglutamyl-4-cyclohexyl-9-carboxamide-2-oxo-bicyclo[4.3.0]non-2-ene]. βCH-TRH [(6R,9S,12S)-1-Aza-3-aminopyroglutamyl-4-cyclohexyl-9-carboxamide-2-oxo-bicyclo[4.3.0]non-2-ene]. \*, Chiral carbon. In αCH-TRH, the H points down from the plane of the fused ring system. In βCH-TRH, the H points up from the plane of the fused ring system. The torsional angles are identified:  $\psi_1$ ,  $\phi_2$ ,  $\psi_2$ ,  $\chi_1^2$ ,  $\chi_2^2$ , and  $\psi_3$ .

with the use of an anodic oxidation/ $\text{TiCl}_4$ -induced cyclization/rearrangement sequence that had been developed to make peptide building blocks with the 1-aza-2-oxobicyclo[4.3.0]nonane ring skeleton (18, 19). (Complete details of this synthesis will be described elsewhere.) Cyclohexyl-Ala<sup>2</sup>-TRH was used instead of TRH because the restricted analogues could not be synthesized with histidine at position 2. The stereochemistry of the isomers was assigned by analogy to building blocks with an isopropyl side chain instead of the cyclohexyl group (19).

**Cell studies.** Measurements of receptor binding and inositol phosphate second messenger formation were made in mouse pituitary AtT-20 cells stably expressing mouse TRH-Rs (20) as described previously (5). In brief, competition binding to intact cells was performed for 1 hr at 37° with 1 nM [<sup>3</sup>H][N<sup>7</sup>-methyl-His]TRH and various concentrations of unlabeled TRH analogues. For experiments in which inositol phosphate formation was measured, cells were incubated in medium containing *myo*-[<sup>3</sup>H]inositol for 48–72 hr, and inositol phosphate formation was measured during a 60-min incubation with various concentrations of TRH or TRH analogues in the presence of 10 mM LiCl. Curves were fitted through nonlinear regression analysis with the use of the PRISM program (GraphPad).

**Simulations.** The structures of cyclohexyl/Ala<sup>2</sup>-TRH and the two restricted analogues, αCH-TRH and βCH-TRH, were built in MacroModel (21) and optimized with the AMBER\* force field (22–24). The main part of the structures of the restricted analogues is attached to the cyclohexyl ring in an equatorial conformation. The optimized structures of αCH-TRH and βCH-TRH are similar, but they prefer oppositely puckered prolines. The conformational popu-

lations of each structure were studied through a two-stage Monte Carlo biased sampling technique recently described by Guarnieri and Wilson (25). The molecules were first subjected to Monte Carlo simulated annealing (26) in MacroModel with the Generalized Born/Surface Area solvation model (27). Mean field population distributions of the torsional angles collected from the simulated annealings were used to construct a mapping of the random numbers into torsional populations (Conformational Memories) so that unpopulated areas are excluded from sampling (25). Each simulated annealing consisted of 16 cooling cycles that started at 800°K and decreased in 10 steps to 310°K, with a temperature protocol of  $T_{n+1} = 0.9 \cdot T_n$ . Fifty thousand Monte Carlo steps were computed at each temperature, resulting in a total of  $8 \times 10^6$  steps for each simulated annealing. The variables in the simulations were the six free torsional angles in cyclohexyl/Ala<sup>2</sup>-TRH and four in the restricted analogues. Two angles were changed simultaneously at each step by a random value between  $-180^\circ$  and  $180^\circ$ . The bond lengths and bond angles were kept constant. In the second part of the simulation, the Conformational Memories guided the collection of 1000 structures from a Monte Carlo simulation of 500,000 steps at 310°K. The structures were clustered according to their pairwise root-mean-square differences with the use of the program Xcluster (28) for structural comparisons.

## Results and Discussion

The structures of TRH and cyclohexyl/Ala<sup>2</sup>-TRH are shown in Fig. 1A. The two conformationally restricted analogues, αCH-TRH and βCH-TRH, are cyclic derivatives of cyclohexyl/Ala<sup>2</sup>-TRH (Fig. 1B). In the restricted analogues, the torsional angles between C<sub>α</sub> of cyclohexylalanine and the peptide carbonyl ( $\psi_2$ ) and between C<sub>α</sub> and C<sub>β</sub> of cyclohexylalanine ( $\chi_1^2$ ) were restricted by a lactam ring, and the peptide bond between cyclohexylalanine and Pro-NH<sub>2</sub> was *trans* (Fig. 1). The only difference between αCH-TRH and βCH-TRH is that they are stereoisomeric at the δ carbon of the proline ring.

We measured the biological activities of the restricted analogues and compared them with unrestricted cyclohexyl/Ala<sup>2</sup>-TRH and TRH (Table 1). All analogues stimulated inositol phosphate second messenger formation to the same maximal extent as TRH (Fig. 2). The unrestricted cyclohexyl/Ala<sup>2</sup> analogue had a 650-fold lower affinity than TRH for

**TABLE 1**  
**Biological activities of TRH, cyclohexyl/Ala<sup>2</sup>-TRH, αCH-TRH, and βCH-TRH**

	$K_i^a$	$\text{EC}_{50}^a$
	nM	
TRH	10 <sup>b</sup>	1 (0.95–1.3)
Cyclohexyl/Ala <sup>2</sup> -TRH	6,500 (5,400–7,900)	430 (380–480)
αCH-TRH	290,000 (220,000–370,000)	44,000 (37,000–52,000)
βCH-TRH	1,900 (1,600–2,200)	91 (76–110)

\* Measured as described in Materials and Methods. Values are mean (95% confidence interval).

<sup>b</sup> From Ref. 1.

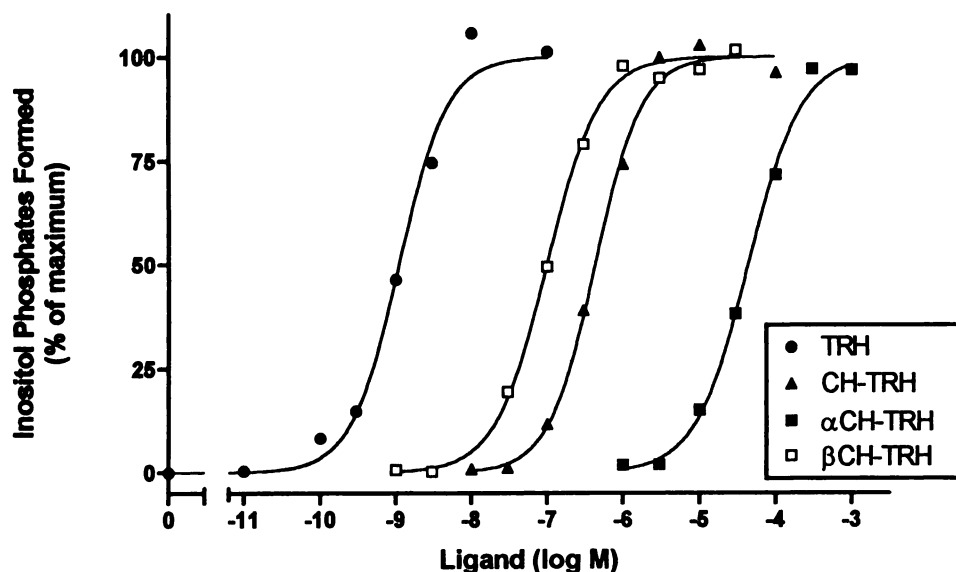


**Fig. 2.** Stimulation of inositol phosphate formation by TRH, cyclohexyl/Ala<sup>2</sup>-TRH,  $\alpha$ CH-TRH, or  $\beta$ CH-TRH. The maximal level of stimulation of inositol phosphate formation was similar for all TRH analogues and was set at 100% in each experiment; stimulation ranged from 4- to 11-fold above basal. Data points represent mean values of duplicate or triplicate determinations in three or four experiments.

TRH-R and was 430-fold less potent than TRH in stimulating inositol phosphate formation. This decrease in binding affinity reflects the importance of histidine at the second position of TRH. Importantly, a model of the unrestricted analogue predicts that the cyclohexyl/Ala<sup>2</sup> residue at the second position does not affect the position of <glutamate relative to Pro-NH<sub>2</sub> (see below). Restricted analogue  $\alpha$ CH-TRH showed further reductions in affinity (45-fold) and potency (100-fold) compared with unrestricted cyclohexyl/Ala<sup>2</sup>-TRH. In contrast, restricted analogue  $\beta$ CH-TRH exhibited a higher affinity (3.4-fold) and was more potent (4.7-fold) than the unrestricted analogue. This enhanced ability of  $\beta$ CH-TRH to interact with TRH-R relative to cyclohexyl/Ala<sup>2</sup>-TRH was observed even though it contains a methylene bridge and fused ring, adding steric bulk that by itself likely reduces the affinity of interaction with TRH-R. Thus, the constraint introduced in  $\beta$ CH-TRH selected a preferred conformation for interaction with the receptor.

To delineate the preferred conformation of the restricted analogues, we used a biased sampling Monte Carlo method (see Materials and Methods). The results from the first part of the conformational search show the distributions of torsional angles of  $\alpha$ CH-TRH and  $\beta$ CH-TRH as a function of temperature (Fig. 3). Each three-dimensional graph has temperature on the x-axis (800–310°K), angle values on the y-axis (–180°–180°), and the fractional population on the z-axis. This analysis confirms that the analogues are conformationally restricted and shows that the major difference between them is in the value of  $\phi_2$ . In both, the  $\phi_2$  distribution is bimodal and well localized, with peaks at  $\pm 60^\circ$ . The two populations are present at high temperatures but converge at 310°K to  $60^\circ$  in  $\alpha$ CH-TRH and to a major population at  $-60^\circ$  with a minor one at  $60^\circ$  in  $\beta$ CH-TRH. There also are small differences in the distribution of  $\psi_3$ . The major population is at  $160^\circ$  and the minor population is at  $-20^\circ$ ; compound  $\beta$ CH-TRH also shows a population at  $70^\circ$ . The populations of  $\psi_1$  and  $\chi_2^2$  are nearly identical in the two compounds.

To compare the conformations of  $\alpha$ CH-TRH and  $\beta$ CH-TRH, an ensemble of structures was produced in the second part of

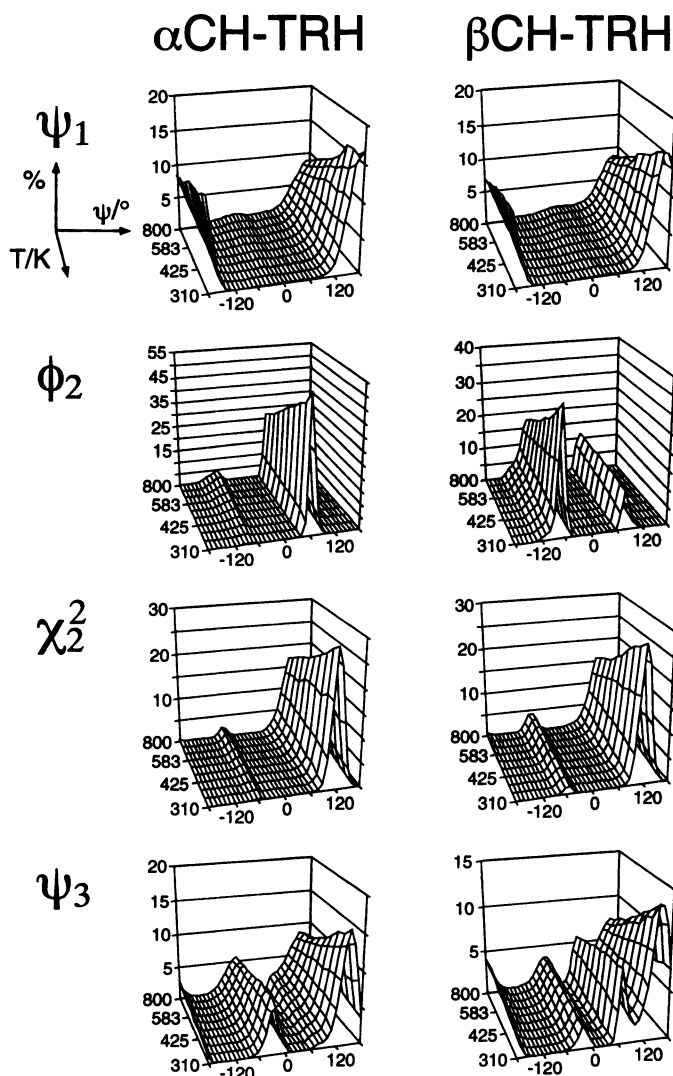


**Fig. 3.** Populated conformational spaces of  $\alpha$ CH-TRH (left) and  $\beta$ CH-TRH (right). The x-axis is temperature (degrees Kelvin), the y-axis is the dihedral angle ( $^\circ$ ), and the z-axis is the percent of the population (%).



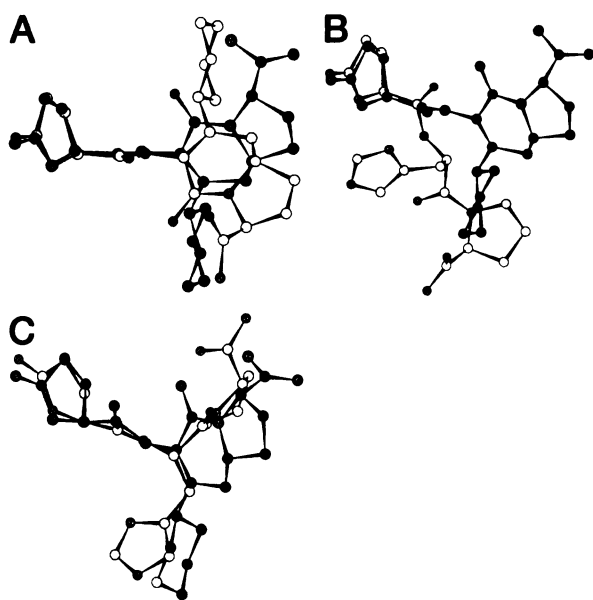


**Fig. 4.** Comparisons of computer-simulated conformations of  $\alpha$ CH-TRH (A), *trans*-TRH (B), and *trans*-TRH in the binding pocket of TRH-R (C) with  $\beta$ CH-TRH. The conformations of *trans*-TRH,  $\alpha$ CH-TRH, and  $\beta$ CH-TRH were simulated in water. The conformers have been aligned so that the <glutamate moieties are superimposed. ●,  $\beta$ CH-TRH; ○,  $\alpha$ CH-TRH (A), *trans*-TRH (B), and *trans*-TRH in the binding pocket of TRH-R (C). Stippled circles, nitrogen atoms; striped circles, oxygen atoms (see text).

the simulation based on the mean field probabilities of all rotatable dihedral angles (Fig. 4). The structures were clustered according to their pairwise root-mean-square deviations into conformational families (28). The torsional angles of the predominant conformations are shown in Table 2. Variations from these angles are so small that the restricted analogues can be assumed to behave similarly in water and inside the receptor. As described above, the major difference between the restricted analogues is in the value of  $\phi_2$ . The value of  $\psi_2$  in the two analogues differs by only  $26^\circ$  and is the result of the different puckering of the proline ring. Because the interaction of a ligand with the TRH-R depends on the relative positioning of the <glutamate and the Pro-NH<sub>2</sub> groups (5, 29), the most probable structures were superimposed on each other, with <glutamate as the reference residue (Fig. 4). The effect of changing  $\phi_2$  from  $-60^\circ$  to  $+60^\circ$  had a large effect on the relative positioning of the remainder of the molecule with respect to the <glutamate (Fig. 4A). The different values of  $\phi_2$  result in opposite orientations of the cyclohexyl rings and the terminal carboxamides. It is important to note that in the sample of 1000 structures of  $\alpha$ CH-TRH, none was in the conformation of  $\beta$ CH-TRH, setting the

probability of  $\alpha$ CH-TRH adopting the conformation of the predominant form of  $\beta$ CH-TRH to  $\leq 1:1000$ .

To understand the increased potency of  $\beta$ CH-TRH, we compared its structure with that of TRH. Superposition of the <glutamate portions of TRH and  $\beta$ CH-TRH (Fig. 4B) shows that the prevalent conformations in solution are very different. Not only are the backbones different, but also the terminal carboxamides are far apart. We modeled the structure of TRH in a computer simulation of the TRH-R binding pocket, which is predicted to be the core of a transmembrane bundle of seven  $\alpha$  helices (5, 29). The superposition of TRH from the model of the TRH/TRH-R complex on  $\beta$ CH-TRH (Fig. 4C) shows an excellent overlap of the backbone, a similar position of the cyclohexyl and histidine moieties, and a good positioning of the terminal carboxamide that could be refined simply by a rotation around  $\psi_3$ . In contrast,  $\alpha$ CH-TRH (Fig. 4A) and TRH from the model of the TRH/TRH-R complex (Fig. 4C) do not superimpose well. Thus, the conformations of the more biologically active restricted analogue,  $\beta$ CH-TRH, in solution and of TRH in the model of the binding pocket are similar, whereas those of TRH in solution and TRH in the binding pocket are different. It is possible that cyclohexyl/Ala<sup>2</sup>-TRH binds to TRH-R differently than TRH and therefore may not simulate the conformation of TRH in the TRH-R binding pocket. We think this is unlikely because cyclohexyl/Ala<sup>2</sup>-TRH is fully active and superimposable on TRH. We conclude that a biologically active conformation of TRH is better represented by  $\beta$ CH-TRH than by  $\alpha$ CH-TRH and that TRH in a model of the TRH/TRH-R complex represents a biologically active conformation. A general corollary to these findings is that conformational data of flexible peptides in solution may not be readily transferred to the peptide/receptor complex.

In our previous studies, we used a combination of experimental analysis of the binding and activation of a series of TRH analogues in native and mutant TRH-Rs and computer simulations to construct a three-dimensional model of the TRH/TRH-R complex at an atomic level of detail (5, 29). Direct contacts were identified through hydrogen bonding and van der Waals interactions between residues in transmembrane helices 3, 6, and 7 of TRH-R and distinct moieties of TRH. Specifically, interactions were described between the <glutamate residue of TRH and Tyr<sup>106</sup> and Asn<sup>110</sup> in helix 3 of TRH-R, between histidine of TRH and Tyr<sup>282</sup> in helix 6, and between the carboxamide of Pro-NH<sub>2</sub> and Arg<sup>306</sup> in helix 7. The model also predicted an interaction between Arg<sup>306</sup> and the peptide carbonyls of TRH, but these have not been tested. We noticed that the conformation of TRH in the complex was different from the structure of *trans*-TRH in solution. For example, the peptide backbone was not ex-

TABLE 2

Comparison of the torsional angles of the predominant conformations of cyclohexyl/Ala<sup>2</sup>-TRH, *trans*-TRH in a crystal,  $\alpha$ CH-TRH,  $\beta$ CH-TRH, and *trans*-TRH in the model of the TRH/TRH-R complex

	$\psi_1$	$\phi_2$	$\psi_2$	$\chi_2^1$	$\chi_2^2$	$\psi_3$	Population %
Cyclohexyl/Ala <sup>2</sup> -TRH	180	120	-140	60	$\pm 60$	180	94
<i>trans</i> -TRH in a crystal	146	-70	137	-163	-71	154	100
$\alpha$ CH-TRH	160	60	-165	0	120	160	89
$\beta$ CH-TRH	160	-60	169	0	120	160	82
<i>trans</i> -TRH in TRH/TRH-R complex	138	-110	-63	174	-167	-99	N.A.

N.A. = not applicable.

tended in TRH in the complex as it is in *trans*-TRH in solution; rather, it assumed a helical turn (Table 2). In this study, we provided evidence that the more active analogue ( $\beta$ CH-TRH) restricts the <glutamate and Pro-NH<sub>2</sub> to relative positions that are superimposable with the positions of these residues in TRH in the TRH/TRH-R complex. We think this is important because it provides an independent test of the accuracy of the model. The conformation of TRH in the TRH-R binding pocket, therefore, likely represents a biologically active TRH conformer because experimental support for the model includes measurements of binding affinity and potency of activation. We suggest that the three-dimensional model may be an accurate representation of the form of the binding pocket in the activated state of TRH-R. It will, of course, require a model that includes the intracellular domains to provide an understanding of the activated state of the receptor because it is the intracellular loops of GPCRs that couple to G proteins to transduce the signal (30).

## References

1. Straub, R. E., G. C. Frech, R. H. Joho, and M. C. Gershengorn. Expression cloning of a cDNA encoding the mouse pituitary thyrotropin-releasing hormone receptor. *Proc. Natl. Acad. Sci. USA* **87**:9514-9518 (1990).
2. Strader, C. D., T. M. Fong, M. P. Graziano, and M. R. Tota. The family of G-protein-coupled receptors. *FASEB J.* **9**:745-754 (1995).
3. Maloneyhuss, K., and T. P. Lybrand. Three-dimensional structure for the  $\beta_2$  adrenergic receptor protein based on computer modeling studies. *J. Mol. Biol.* **225**:859-871 (1992).
4. Mouillac, B., B. Chini, M.-N. Balestre, J. Elands, S. Trumpp-Kallmeyer, J. Hoflack, M. Hibert, S. Jard, and C. Barberis. The binding site of neuropeptide vasopressin V1a receptor: evidence for a major localization within transmembrane regions. *J. Biol. Chem.* **270**:25771-25777 (1995).
5. Perlman, J. H., L. Laakkonen, R. Osman, and M. C. Gershengorn. A model of the thyrotropin releasing hormone (TRH) receptor binding pocket: evidence for a second direct interaction between transmembrane helix 3 and TRH. *J. Biol. Chem.* **269**:23383-23386 (1994).
6. Baldwin, J. M. The probable arrangement of the helices in G protein-coupled receptors. *EMBO J.* **12**:1693-1703 (1993).
7. Schertler, G. F. X., C. Villa, and R. Henderson. Projection structure of rhodopsin. *Nature (Lond.)* **362**:770-772 (1993).
8. Baldwin, J. M. Structure and function of receptors coupled to G proteins. *Curr. Opin. Cell Biol.* **6**:180-190 (1994).
9. Gershengorn, M. C., and R. Osman. Molecular and cellular biology of thyrotropin-releasing hormone (TRH) receptors. *Physiol. Rev.* **76**: 175-191 (1996).
10. Kamiya, K., M. Takamoto, Y. Wada, M. Fujino, and M. Nishikawa. Molecular conformation of thyrotropin-releasing hormone from the X-ray structural analysis of its tartrate. *J. Chem. Soc. Chem. Commun.* **10**:438-439 (1980).
11. Deslauriers, R., C. Garrigou-Lagrange, A.-M. Bellocq, and I. C. P. Smith. Carbon-13 nuclear magnetic resonance studies on thyrotropin-releasing factor and related peptides. *FEBS Lett.* **31**:59-66 (1973).
12. Donzel, B., M. Goodman, J. Rivier, N. Ling, and W. Vale. Synthesis and conformations of hypothalamic hormone releasing factors: two TRF-analogues containing backbone N-methyl groups. *Nature (Lond.)* **256**:750-751 (1975).
13. Montagut, M., B. Lemanceau, and A.-M. Bellocq. Conformational analysis of thyrotropin releasing factor by proton magnetic resonance spectroscopy. *Biopolymers* **13**:2615-2629 (1974).
14. Unkefer, C. J., R. D. Walker, and R. E. London. Hydrogen-1 and carbon-13 nuclear magnetic resonance conformational studies of the His-Pro peptide bond: conformational behaviour of TRH. *Int. J. Peptide Protein Res.* **22**: 582-589 (1983).
15. Vicar, J., E. Abillon, F. Toma, F. Pirou, K. Litner, K. Blaha, P. Fromageot, and S. Fermandjian. The two conformations of TRH in solution. *FEBS Lett.* **97**:275-278 (1979).
16. Perlman, J. H., C. N. Thaw, L. Laakkonen, C. Y. Bowers, R. Osman, and M. C. Gershengorn. Hydrogen bonding interaction of thyrotropin-releasing hormone (TRH) with transmembrane tyrosine 106 of the TRH receptor. *J. Biol. Chem.* **269**:1610-1613 (1994).
17. Perlman, J. H., L. Laakkonen, R. Osman, and M. C. Gershengorn. Distinct roles for arginines in transmembrane helices 6 and 7 of the thyrotropin-releasing hormone receptor. *Mol. Pharmacol.* **47**:480-484 (1995).
18. Moeller, K. D., C. E. Hanau, and A. d'Avignon. The use of HMQC-TOCSY experiments for elucidating the structures of bicyclic lactams: uncovering a surprise rearrangement in the synthesis of a key Phe-Pro building block. *Tetrahedron Lett.* **35**:825-828 (1994).
19. Li, W., C. E. Hanau, A. d'Avignon, and K. D. Moeller. Conformationally restricted peptide mimetics: the incorporation of 6,5-bicyclic lactam ring skeletons into peptides. *J. Org. Chem.* **60**:8155-8170 (1995).
20. Matus-Leibovitch, N., D. R. Nussenzveig, M. C. Gershengorn, and Y. Oron. Truncation of the thyrotropin-releasing hormone carboxyl tail causes constitutive activity and leads to impaired responsiveness in *Xenopus* oocytes and AtT20 cells. *J. Biol. Chem.* **270**:1041-1047 (1995).
21. Mohamadi, F., N. G. J. Richards, W. C. Guida, R. Liskamp, M. Lipton, C. Cauffield, G. Chang, T. Hendrickson, and W. C. Still. MacroModel: an integrated software system for modeling organic and bioorganic molecules using molecular mechanics. *J. Comp. Chem.* **11**:440-467 (1990).
22. Weiner, P. K., and P. A. Kollman. AMBER: assisted model building with energy refinement: a general program for modeling molecules and their interactions. *J. Comp. Chem.* **2**:287-303 (1981).
23. Weiner, S. J., P. A. Kollman, D. A. Case, U. C. Singh, C. Ghio, G. A. Alagona, S. J. Profeta, and P. Weiner. A new force field for molecular mechanical simulation of nucleic acids and proteins. *J. Am. Chem. Soc.* **106**:765-784 (1984).
24. McDonald, Q. D., and W. C. Still. AMBER\* torsional parameters for the peptide backbone. *Tetrahedron Lett.* **33**:7743-7746 (1992).
25. Guarnieri, F., and S. R. Wilson. Conformational Memories and a simulated annealing program that learns: application to LTB<sub>4</sub>. *J. Comp. Chem.* **16**:648-653 (1995).
26. Kirkpatrick, S., C. D. Gelatt, Jr., and M. P. Vecchi. Optimization by simulated annealing. *Science (Washington D. C.)* **220**:671-680 (1983).
27. Still, W. C., A. Tempczyk, R. C. Hawley, and T. Hendrickson. Semianalytical treatment of solvation for molecular mechanics and dynamics. *J. Am. Chem. Soc.* **112**:6127-6129 (1990).
28. Shenkin, P. S., and D. Q. McDonald. Cluster analysis of molecular conformations. *J. Comp. Chem.* **15**:899-916 (1994).
29. Perlman, J. H., L. Laakkonen, L. J., Guarnieri, F., Osman, R. and Gershengorn, M. C. A refined model of the thyrotropin-releasing hormone (TRH) receptor binding pocket. Experimental analysis and energy minimization of the complex between TRH and TRH receptor. *Biochemistry* **35**: in press.
30. Strader, C. D., T. M. Fong, M. R. Tota, D. Underwood, and R. A. F. Dixon. Structure and function of G protein-coupled receptors. *Annu. Rev. Biochem.* **63**:101-132 (1994).

Send reprint requests to: Dr. Marvin C. Gershengorn, Cornell University Medical College, 1300 York Avenue, Room A328, New York, NY 10021.